Bright photoactivatable fluorophores for single-molecule imaging

Jonathan B. Grimm,† Brian P. English,† Heejun Choi, Anand K. Muthusamy, Brian P. Mehl, Peng Dong, Timothy A. Brown, Jennifer Lippincott-Schwartz, Zhe Liu, Timothée Lionnet,* Luke D. Lavis*

Janelia Research Campus, Howard Hughes Medical Institute, 19700 Helix Drive, Ashburn, Virginia 20147, USA

†These authors contributed equally

*Corresponding authors' email: lionnett@janelia.hhmi.org; lavisl@janelia.hhmi.org

ABSTRACT: Small molecule fluorophores are important tools for advanced imaging experiments. The development of self-labeling protein tags such as the HaloTag and SNAP-tag has expanded the utility of chemical dyes in live-cell microscopy. We recently described a general method for improving the brightness and photostability of small, cell-permeable fluorophores, resulting in the novel azetidine-containing "Janelia Fluor" (JF) dyes. Here, we refine and extend the utility of the JF dyes by synthesizing photoactivatable derivatives that are compatible with live-cell labeling strategies. These compounds retain the superior brightness of the JF dyes once activated, but their facile photoactivation also enables improved single-particle tracking and localization microscopy experiments.

Small-molecule fluorophores are brighter than fluorescent proteins and remain a crucial element of modern microscopy methods.[1,2] The development of new protein-specific labeling strategies, such as the self-labeling tag concept pioneered by Johnsson,[3,4] enables the formation of fluorescent bioconjugates inside living cells: bright, membrane-permeable synthetic dyes passively diffuse into cells where they form covalent bonds with their genetically-encoded cognate protein fused to a factor of interest. Self-labeling tags thus combine genetic encoding—one of the main advantages of fluorescent proteins—with the favorable photophysics of organic fluorophores. Building upon these sophisticated attachment techniques, we recently reported that incorporation of four-membered azetidine rings could substantially improve the brightness and photostability of small, cell-permeable fluorophores.[5] These "Janelia Fluor" (JF) dyes are excellent labels for live-cell imaging, especially in single-molecule tracking experiments where the improved brightness and photon counts allowed longer observations and better localization of individual fluorescent conjugates. We now report photoactivatable (PA) versions of JF_{549} and JF_{646}, demonstrate their compatibility with existing live-cell labeling strategies, and show their utility in single-molecule tracking and super-resolution imaging.

Our laboratory has developed efficient synthetic strategies to prepare photoactivatable rhodamines by N-acylation with standard photolabile "cages".[6,7] Most caging groups are large and hydrophobic, however, which diminishes solubility and reactivity with self-labeling tag proteins. Moreover, classic photocaging strategies are incompatible with fully N-alkylated rhodamine dyes such as Janelia Fluor 549 and Janelia Fluor 646. To circumvent these issues, we utilized a caging strategy serendipitously discovered by Hell and coworkers, in which treatment of rhodamine dyes with oxalyl chloride and diazomethane generates a spirocyclic diazoketone that is colorless and nonfluorescent.[8,9] Activation of these diazoketone dyes with short-

wavelength light yields a fluorescent species as the major product. Although diazoketone-caged dyes have been employed as antibody labels for fixed cell imaging, this type of photoactivatable dye has not been incorporated into self-labeling tag systems nor used in live-cells.

To test the compatibility of this caging strategy with the azetidinyl Janelia Fluor dyes, we first prepared the photoactivatable JF_{549} (PA-JF_{549}, **2**) in good yield from JF_{549}[5] (**1**, **Fig. 1a**). We then evaluated the photochemistry of PA-JF_{549} (**2**) in aqueous solution; previous reports had only described the photolysis of diazoketone-caged dyes in methanol.[8,9] Surprisingly, the major product from exhaustive photolysis of compound **1** in aqueous solution was not the expected phenylacetic acid dye **3** but rather the methyl-substituted JF_{549} (**4**) along with the putative nonfluorescent "dark product" **5** (**Fig. 1a**). Compound **4** was generated with an apparent photochemical quantum yield (Φ_{PC}) value of 2.2% (**Supplementary Note**), similar to photoswitchable fluorescent proteins ($\Phi_{PC} \approx 1\%$).[10] This unexpected product is due to efficient ($\Phi_{PC} = 15\%$) photoinduced decarboxylation[11] of the initial photochemical product **3** (**Supplementary Note**). Nevertheless, the two photoproducts **3** and **4** are highly fluorescent molecules with similar spectral properties to the parent JF_{549} (**1**; **Fig. 1b**). As reported before,[5] fluorophore **1** exhibits an absorption maximum (λ_{max}) of 549 nm, extinction coefficient (ε) of 1.01×10^5 $M^{-1}cm^{-1}$, emission maximum (λ_{em}) of 571 nm, and a fluorescence quantum yield (Φ_F) of 0.88. Fluorophore **3** showed $\lambda_{max}/\lambda_{em}$ = 553 nm/573 nm and retained 95% of the brightness of **1** ($\varepsilon = 9.89 \times 10^4$ $M^{-1}cm^{-1}$; $\Phi_F = 0.85$) whereas dye **4** gave $\lambda_{max}/\lambda_{em}$ = 551 nm/570 nm and retained 75% of the brightness of **1** ($\varepsilon = 8.59 \times 10^4$ $M^{-1}cm^{-1}$; $\Phi_F = 0.78$).

Given the brightness of the PA-JF_{549} photoproducts we then synthesized the HaloTag ligand[12] of PA-JF_{549} (**6**, **Fig. 1c**, **Supplementary Note**). Labeling of HaloTag protein with **6** either *in vitro*, in live cells, or in fixed cells gave conjugates with low background absorption and

fluorescence that could be activated by one- or two-photon illumination (**Supplementary Fig. 1a, Supplementary Videos 1–3**). We found attachment of **6** to the HaloTag improves the yield of the desired fluorescent products by two-fold compared to the free PA-JF_{549} ligand (**Supplementary Fig. 1b,c**), perhaps by restricting conformational flexibility and preventing the formation of the planar dark product **5** (**Fig. 1a**; **Supplementary Note**). This enhancement in desired photochemical outcome upon conjugation to protein was also observed for the PA-JF_{549} SNAP-tag ligand (**7**, **Fig. 1c**, **Supplementary Fig. 1d–f**). Although advantageous, this improvement in photochemistry upon conjugation does not eliminate the need for washing out free ligand.

We directly compared the performance of the PA-JF_{549}-HaloTag ligand (**6**) to the genetically encoded mEos3.2 in single-particle tracking photoactivated localization microscopy (sptPALM)[13] experiments in mouse embryonic stem (ES) cells expressing either HaloTag–Sox2 or mEos3.2–Sox2 fusions (**Fig. 1d**, **Supplementary Video 4**). The PA-JF_{549} showed a large improvement in both the brightness and photostability compared to the mEos3.2 fluorophore.[14] The PA-JF_{549} ligand (**6**) gave higher photons/particle/frame (median = 120.7) and longer tracks (mean = 0.20 s) than mEos3.2 (median photons/particle/frame = 70.9; mean track length = 0.07 s; **Fig. 1e,f**). We also compared ligand **6** to the commercially available tetramethylrhodamine (TMR) HaloTag ligand[12] (**9**, **Supplementary Fig. 1b,g**) using a multifocus microscope (MFM)[15] setup where we observed superior performance of the PA-JF_{549} ligand in 3D tracking (**Supplementary Fig. 1h–l**, **Supplementary Video 5**).

Given the performance enhancement compared to mEos3.2 in live-cell sptPALM, we then tested the utility of PA-JF_{549} HaloTag ligand as a label for PALM in fixed cells. We first compared localization microscopy of the mitochondrial protein TOMM20 fused to either

mEos3.2 (**Supplementary Fig. 1m**) or the HaloTag protein and labeled with ligand **6** (**Fig. 1g**). The PA-JF_{549}-HaloTag conjugate showed only modest blinking (**Supplementary Note**) and gave substantially higher photon counts per localization event per frame (median = 636.6) and calculated localization precision (median σ = 13.5 nm) compared to mEos3.2 (median photons/localization/frame = 266.8; median σ = 20.2 nm; **Fig. 1h,i**). We also confirmed the dyes could function as PALM labels with other HaloTag fusions in different cellular regions (**Supplementary Fig. 1n–p**, **Supplementary Video 6**).

We then set out to perform two-color sptPALM, an experiment that has been stymied by the scarcity of two spectrally distinct photoactivatable fluorophores. We reasoned that the use of the same diazoketone caging strategy on different Janelia Fluor dyes could allow sparse photoactivation of both labels with similar efficiency, thus facilitating two-color experiments. We first converted JF_{646} (**11**) into the photoactivatable Janelia Fluor 646 (PA-JF_{646}, **12**, **Supplementary Fig. 2a**, **Supplementary Note**) to test whether this caging strategy would be compatible with the Si-rhodamine scaffold. Interestingly, photolysis of the free PA-JF_{646} **12** gave only small amounts (<5%) of the expected fluorescent products **13** and **14,** with the major product being the nonfluorescent **15** (**Supplementary Fig. 2a**, **Supplementary Note**). Nevertheless, the "on-protein" improvement in photochemistry observed for the PA-JF_{549} compounds (**Supplementary Fig. 1a–f**) led us to predict that PA-JF_{646} would show better performance as a photoactivatable fluorophore when conjugated. Accordingly, we synthesized the HaloTag and SNAP-tag ligands of PA-JF_{646} (**16** and **17**, respectively; **Fig. 2a**, **Supplementary Note**). These compounds showed up to a five-fold improvement in photochemical outcome upon binding to their cognate protein (**Supplementary Fig. 2b–e**, **Supplementary Note**). The low background staining exhibited with PA-JF_{549} ligand **6** was also

observed with the PA-JF_{646} HaloTag ligand **16** (**Supplementary Fig. 2f,g**) allowing facile sptPALM in live cells (**Fig. 2b**, **Supplementary Video 7**).

To further validate the PA-JF_{549} and PA-JF_{646} pair for two-color sptPALM we expressed the transcription factor Sox2 as a fusion with HaloTag protein and labeled with PA-JF_{549}-HaloTag ligand **6**. We coexpressed histone H2B as a fusion with the SNAP-tag and labeled this population with PA-JF_{646}-SNAP-tag ligand (**17**); these photoactivatable dyes allowed simultaneous tracking of both H2B and Sox2 by photoactivation with 405 nm light. We generated a map of histone H2B location using a standard PALM analysis (**Fig. 2c**) and used it to define Sox2 trajectories that were either colocalized or not colocalized with this chromatin marker (**Fig. 2d**). As expected, the molecules of Sox2 that were colocalized with histone H2B exhibited slower diffusion coefficients than the non-colocalized fraction (**Fig. 2e–g**, **Supplementary Fig. 2h,i**).

Finally, we investigated the PA-JF_{646} label for multicolor localization microscopy. Although a few self-labeling tag ligands have been used for PALM imaging,[9,16,17] previously reported molecules exhibit relatively short emission maxima, and are thus incompatible with other localization microscopy labels such as photoconvertible fluorescent proteins. Based on our previous work with another caged Si-rhodamine with similar wavelengths,[6] we reasoned that PA-JF_{646} would be red-shifted enough to be useful for two-color PALM with the photoconvertable protein mEos3.2.[14] We first showed that PA-JF_{646}-HaloTag ligand **16** could be used for high-quality one-color PALM in cells expressing HaloTag–vimentin or HaloTag–TOMM20 fusions (**Supplementary Fig. 2j,k**). The calculated localization precision in the TOMM20 image using JF_{646} ligand **16** was similar to JF_{549} (median σ = 13.8 nm) and higher than mEos (20.2 nm; **Fig. 1i**, **Supplementary Fig. 2l**). For a two-color experiment, we expressed the mutant Huntingtin protein Htt-94Q as a fusion protein with mEos3.2 and histone H2B as a fusion

with the HaloTag, labeling with PA-JF_{646}-HaloTag ligand **16**. After labeling, fixation, and two-color PALM (**Fig. 2h**), we observed that histone H2B (magenta) and Htt-94Q aggregates (green) only rarely overlap (i.e., few white spots), which supports the hypothesis that the aggregates formed by expanded polyglutamine domains displace chromatin structures in the nucleus. Notably, the JF_{646} dye was significantly brighter than mEos3.2, emitting nearly seven-fold more photons/localization/frame relative to the fluorescent protein (**Fig. 2h**).

In conclusion, we report photoactivatable versions of the bright, photostable Janelia Fluor dyes. These fluorophores retain the superior photon yields and utility in live cells exhibited by the fluorescent JF dyes but have the added benefit of photoactivation, allowing sophisticated single-particle tracking experiments and facile super-resolution microscopy in different cellular regions. In particular, JF_{646} is the first far-red photoactivatable fluorophore compatible with live-cell labeling using the HaloTag or SNAP-tag systems, allowing multicolor single-particle tracking experiments and super-resolution microscopy with established photoconvertible fluorescent proteins. Unlike traditional photoactivatable xanthene dyes that contain large, poorly soluble caging groups,[6] we expect these small and bright photoactivatable labels to be compatible with many different labeling strategies, therefore extending the boundaries of single-molecule imaging in live and fixed cells. Beyond single molecule imaging, these versatile, membrane-permeable labels should provide a favorable alternative to photoconvertible fluorescent proteins in any live imaging experiment where photoactivation is used to highlight a specific cell or cellular region.

METHODS

Chemical Synthesis and Photochemistry. Experimental details and characterization for all novel compounds and subsequent spectroscopy and photochemistry experiments can be found in the Supplementary Note.

UV–Vis and Fluorescence Spectroscopy. Spectroscopy was performed using 1-cm path length quartz cuvettes. All measurements were taken at ambient temperature (22 ± 2 °C). Absorption spectra were recorded on a Cary Model 100 spectrometer (Agilent). Fluorescence spectra were recorded on a Cary Eclipse fluorometer (Varian). Absolute fluorescence quantum yields (Φ_F) for all fluorophores were measured using a Quantaurus-QY spectrometer (model C11374, Hamamatsu).

General Microscopy Methods. A comprehensive listing of instrument parameters for all imaging experiments can be found in Supplementary Table 1. Additional information is given below.

Cell Culture. Mouse D3 ES cells (ATCC) were maintained on 0.1% w/v gelatin coated plates in the absence of feeder cells. The ES cell medium was prepared by supplementing knockout Dulbecco's modified eagles media (DMEM, Invitrogen) with 15% v/v fetal bovine serum (FBS), 1 mM GlutaMAX, 0.1 mM nonessential amino acids, 1 mM sodium pyruvate, 0.1 mM 2-mercaptoethanol, and 1000 units of leukemia inhibitory factor (LIF; Millipore). U2OS (ATCC) and COS-7 (ATCC) cells were cultured in DMEM (Corning) with 10% v/v fetal bovine serum (FBS) supplemented with 2 mM L-glutamine or 2 mM GlutaMAX. Cells were regularly tested for mycoplasma contamination by the Janelia Cell Culture Facility.

Plasmid Construction. Sox2 and histone H2B cDNA were amplified from ES cell cDNA libraries. Htt-94Q cDNA was obtained from Addgene (Plasmid #23966). The full-length cDNAs

were cloned into the Piggybac transposon vector (PB533A-2, System Biosciences) or a modified Piggybac transposon vector with PuroR. The sequence for HaloTag (Promega) or mEOS3.2 (Addgene: Plasmid #54525) was ligated in-frame with the cDNA of the desired proteins at the N-terminus (HaloTag–Sox2) or C-terminus (histone H2B–HaloTag, histone H2B–SNAP-tag, and Htt-94Q–mEOS3.2-NLS). The plasmids coding ensconsin–HaloTag, clathrin–HaloTag, TOMM20–HaloTag, Sec61β–HaloTag, and vimentin–HaloTag were constructed by substituting the sequence for the HaloTag for the sequence of mEmerald in a collection of plasmids that were a generous gift from Michael Davidson (Florida State). Each plasmid was transiently transfected into U2OS cells using the Nucleofactor Kit (Lonza).

Stable Cell Line Generation. Stable cell lines were generated by co-transfection of Piggybac transposon vector with a helper plasmid that over-expresses Piggybac transposase (Super Piggybac Transposase, System Biosciences). At 48 h post-transfection, cells were subjected to neomycin or puromycin (Invitrogen) selection. Transfection was conducted by using the Nucleofector system (Lonza).

ES Cell Labeling Strategy and Preparation for Imaging. One day before imaging, ES cells were plated onto a cover slip pre-coated with IMatrix-511 (Clontech). Imaging was performed in the ES cell imaging medium, which was prepared by supplementing FluoroBrite medium (Invitrogen) with 10% v/v FBS, 1 mM glutamax, 0.1 mM nonessential amino acids, 1 mM sodium pyruvate, 10 mM HEPES (pH 7.2–7.5), 0.1 mM 2-mercaptoethanol, and 1000 units of LIF (Millipore). For PA-JF_{549} or PA-JF_{646} labeling, cells were incubated with PA-JF_{549}-HaloTag ligand (**6**) or PA-JF_{646}-HaloTag ligand (**16**) at a final concentration of 100 nM for 1 h. For the 2-color sptPALM live-cell tracking experiments, labeled cells were washed with ES cell imaging medium (3×) before imaging. For the 2-color fixed-cell PALM imaging experiments, labeled

cells were washed with PBS (4×), fixed in 4% w/v paraformaldehyde for 10 min and washed with PBS (3×). The final PALM imaging was performed in PBS solution.

3D spt-*d*STORM and spt-PALM tracking experiments. Fluorescently tagged HaloTag–Sox2 molecules labeled either with PA-JF_{549}-HaloTag ligand (**6**) or with TMR-HaloTag ligand (**9**) were tracked in live ES cells in 3D using a custom-built multifocus microscope.[15] The fluorescence from nine focal planes was simultaneously recorded using an iXon Ultra EMCCD camera (DU-897U-CS0-#BV, 17MHz EM amplifiers, pre-amp setting 1, Gain 300) at a frame time of 30 ms.

One-color PALM labeling and fixation. Cells were grown on pre-cleaned 25 mm diameter coverslips or pre-cleaned 25-mm diameter coverslips embedded with containing gold-nanorods as fiducial markers (generous gift of Gleb Shtengel, Janelia). Before fixation, cells were labeled with 10 nM of the HaloTag ligand for 30 min at 37 ˚C, 5% CO_2. Cells were then washed three times with pre-warmed DMEM buffer containing 10% FBS. Before fixation, the coverslips were washed twice with pre-warmed PBS solution without magnesium chloride or calcium chloride. 1 mL of 8% formaldehyde solution in PBS was slowly added to a dish containing 1 mL of PBS, and the resulting 4 % formaldehyde solution was incubated at room temperature for 10 min. The coverslips were washed twice with PBS and incubated in 0.1 % v/v Triton X-100 in PBS solution for 4 min. The coverslips were washed twice in PBS, and then incubated in 1% w/v BSA in PBS for 1 h at ambient temperature. After washing twice more with PBS, the coverslips were mounted into metal cell chambers for PALM imaging.

Two color sptPALM live-cell tracking experiments. ES cells expressing both HaloTag–Sox2 fusions labeled with PA-JF_{549}-HaloTag ligand (**6**) and SNAP-tag–histone H2B fusions labeled with PA-JF_{646}-SNAP-tag ligand (**17**) were tracked simultaneously using a custom-built 3-camera

microscope.[18] Two iXon Ultra EMCCD cameras (DU-897-CS0-BV and DU-897U-CS0-EXF, both cooled to –80 °C, 17MHz EM amplifiers, pre-amp setting 3, Gain 400) were synchronized using a National Instruments DAQ board (NI-DAQ-USB-6363) at a frame time of 10 ms. 5 ms stroboscopic excitations of a 555 nm laser (CL555-1000-O with TTL modulation, CrystaLaser) and a 639 nm laser (Stradus 637-140, Vortran) were synchronized to the frame times of the two respective cameras via LabVIEW 2012 (National Instruments). The two lasers stroboscopically illuminated the sample using peak power densities of ~1.7 kW/cm^2 using HiLo illumination of the nucleus The PA-JF$_{549}$ and PA-JF$_{646}$ labels were photoconverted by 100 µs long excitation pulses of 407 nm light (50 W/cm^2) every second. During the course of image acquisition, the pulse length was increased to 200 µs long pulses. During imaging, cells were maintained at 37 °C and 5 % CO_2 using a Tokai-hit stage top incubator and objective heater.[18] We determined colocalized Sox2 and histone H2B trajectories in our live cell experiment using an analysis published previously.[5,19] Briefly, we localized particles and build trajectories in both channels separately. We then assigned as colocalized trajectories that dwelled within 320 nm of one another for at least 10 ms. We then calculated diffusion coefficients maps and histograms as described in Grimm, English et al.[5]

Determination of Background Staining. COS-7 cells were stably transfected with a plasmid expressing a human H2B-HaloTag protein fusion. Untransfected COS-7 cells and the stable histone H2B–HaloTag expressing cells were plated into 35 mm MatTek glass bottom dishes at 2 × 10^5 cells per plate in phenol red-free DMEM with 10% FBS and GlutaMAX. After 24 h, cells were rinsed with PBS and fixed with 2 mL of fresh 4% w/v paraformaldehyde in 0.1 M phosphate buffer, pH 7.4 for 30 min, followed by two washes with PBS. The histone H2B–HaloTag protein was stained with 100 nM of either PA-JF$_{549}$ HaloTag ligand (**6**) or PA-JF$_{646}$

HaloTag ligand (**16**) for 30 min, along with 5 μg/mL Hoechst 33342 (Invitrogen) in PBS. The cells were then washed twice with PBS, washed for 20 min with PBS containing 0.1% v/v Triton X-100 and 3% w/v BSA, followed by two more washes with PBS. Cells were imaged using a Zeiss 710 LSM. Z-dimension stack boundaries were set using the Hoechst 33342 nuclear reference stain, which was imaged using 405 nm excitation and 410–485 nm emission. Partial photoactivation of PA-JF_{549} and PA-JF_{646} was accomplished with 60 iterations of 405 nm set at 75% laser power. Images for activated JF_{549} were collected using 561 nm excitation and 566–685 nm emission. Images for JF_{646} were collected using 633 nm excitation and 638–759 nm emission. The Hoechst 33342 and JF-dye tracks were collected separately. Image analysis was done using Fiji. Confocal stacks are displayed as maximum projection images. The experimental and control images were set to the same brightness/contrast scales.

Two-color fixed-cell PALM imaging acquisition. ES cells expressing both Htt94Q–mEOS3.2 and HaloTag–histone H2B labeled with PA-JF_{646}-HaloTag ligand (**16**) were imaged using the previously described custom-built 3-camera microscope at a frame time of 50 ms and a constant illumination power density of around 4 kW/cm^2 for both 555 nm and 639 nm excitation lasers. mEos3.2 and PA-JF_{646} were photoconverted by 100 μs long excitation pulses of 407 nm light (100 W/cm^2) every second. The mEos3.2 emitted 115.6 photons/localization/frame and molecules emit on average for 4 frames, as determined by tracking using stringent displacement parameters to select immobile particles. Thus, each mEos3.2 emits approximately 460 photons, consistent with literature reports.[20] The 1.7-fold higher resolution enhancement afforded by JF_{646} is smaller than expected based on the 6.5-fold more photons/localization/frame (757.6) and the red-shifted spectra of JF_{646}. This is primarily due to the camera pixel size being optimized for the

dimmer protein fluorophore and the increased fluorescence background generated by bright out-of-focus JF_{646} molecules.

PALM and sptPALM tracking image analysis. For simultaneous 2-camera imaging and tracking, the two 16-bit TIFF stacks were registered using the similarity (2d) transformation model using a descriptor-based Fiji plugin.[21] Super-resolution images were rendered using the software package Localizer by Dedecker *et al.*[22] with 8-way adjacency particle detection, 20 GLRT sensitivity, and a PSF of 1.3 pixels. The following settings were chosen for particle track linking: 5 pixel maximum jump distance, 3-frame minimum track length, and 15 GLRT sensitivity. Resulting tracks were then exported as text files, and diffusion mapping was performed with code written in Igor Pro 6.36 (WaveMetrics). The code calculates local apparent diffusion coefficients evaluated in 20 nm by 20 nm grids from the mean square displacements over the frame-time timescale.[23] Zeiss Zen 2.1 software was used to analyze images taken from Zeiss Elyra microscope.

Multifocus image processing. We assembled 3D stacks by aligning the nine simultaneously obtained focal planes on top of one another using bead calibration data as described previously.[15] For 3D particle tracking we imported the 16-bit TIFF stack into DiaTrack 3.04 Pro,[24] which identifies and fits the intensity spots with 3D Gaussian function matched to a pre-determined PSF. The following settings were chosen for 3D particle tracking: Subtract background, Filter data of 1.05, PSF of 1.3 pixels, remove dim of 15, and remove blurred of 0.05. Resulting 3D tracks were exported with code written in Igor Pro 6.36 as one text file containing frame numbers, as well as x, y, and z-coordinates of all detected points. We plotted a map of all detected particle locations in the x-y plane, color-coded for height (z), and calculated histograms of detected number of particles over the course of 3D sptPALM data acquisitions. Local

diffusion mapping in the x-z plane was performed with code that calculates local apparent diffusion coefficients evaluated in 20 nm by 20 nm grids and displays the diffusion map as an x–z projection. Integrated fluorescence intensities from particles detected in the central two focal planes (multifocal plane 4 and 5) were calculated and converted to photon counts using analysis routines written in Igor Pro version 6.36.[5] Localization errors were calculated using equation (6) in Mortensen *et al*.[25]

AUTHOR INFORMATION

Corresponding Authors: lionnett@janelia.hhmi.org; lavisl@janelia.hhmi.org

CONFLICT OF INTEREST STATEMENT

The authors declare conflict of interest. J.B.G., B.P.E., A.K.M., Z.L., T.L., and L.D.L. have filed patent applications whose value may be affected by this publication.

FUNDING SOURCES

This work was supported by the Howard Hughes Medical Institute.

ACKNOWLEDGEMENT

We thank Wesley Legant and Eric Betzig (Janelia) for contributive discussions; Helen White, Deepika Walpita, Kathy Schaefer, and Phuong Nguyen (Janelia) for assistance with molecular biology and cell culture; and Adam Berro, Ahmed Abdelfattah, and Eric Schreiter (Janelia) for the purified HaloTag and SNAP-tag proteins.

FIGURE 1

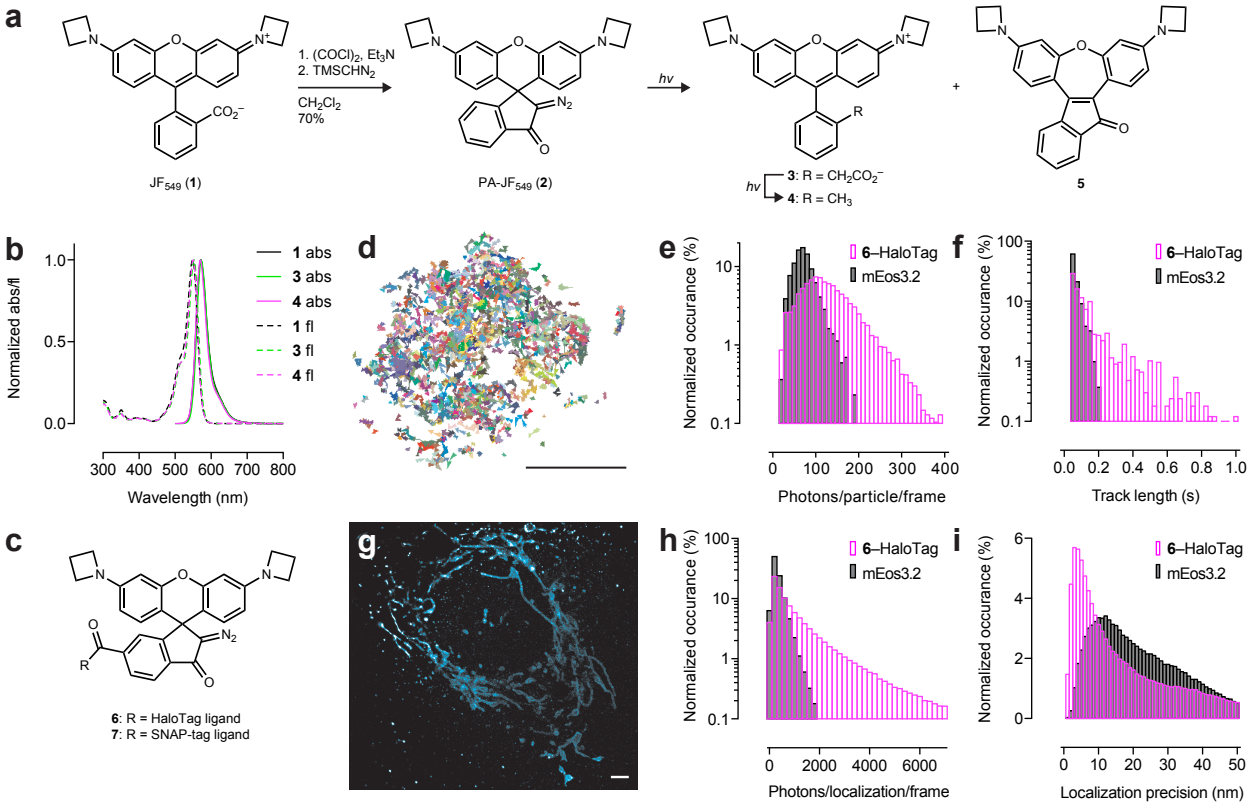

Figure 1. Synthesis, characterization, and utility of photoactivatable Janelia Fluor 549 (PA-JF$_{549}$). (**a**) Synthesis and photochemistry of PA-JF$_{549}$. Treatment of JF$_{549}$ (**1**) with oxalyl chloride and TMS diazomethane yields PA-JF$_{549}$ (**2**). Photoconversion (365 nm) yields only a trace amount of the expected phenylacetic acid derivative (**3**) with methyl-substituted JF$_{549}$ (**4**) as the major product (50%) and the indanone **5** as the minor (10%) product. (**b**) Normalized absorption (abs) and fluorescence emission (fl) of **1**, **3**, and **4**. (**c**) Chemical structure of PA-JF$_{549}$-HaloTag ligand (**6**) and PA-JF$_{549}$-SNAP-tag ligand (**7**). (**d**) Image of cumulative single-particle tracks of Sox2–HaloTag labeled with PA-JF$_{549}$ ligand **6**; scale bar: 5 µm. (**e**) Histogram of normalized occurrence *vs*. photons/particle/frame when performing sptPALM of Sox2 using the **6**–HaloTag fusion (magenta, median = 120.7 photons) or mEos3.2 fusion (black, median = 70.9 photons) under identical imaging conditions. (**f**) Histogram of normalized occurrence *vs*. track length when performing sptPALM of Sox2 using the **6**–HaloTag fusion (magenta, mean = 0.20 s) or mEos3.2 fusion (black, mean = 0.07 s) under identical imaging conditions. (**g**) PALM image of U2OS cell expressing TOMM20-HaloTag and labeled with PA-JF$_{549}$ ligand **6**; The 268,561 detected molecules are displayed according to their localization full-width at half-maximum. The median calculated localization error was 13.5 nm; scale bar: 2 µm. (**h**) Histogram of normalized occurrence *vs*. photons/localization/frame when performing PALM of TOMM20 using the **6**–HaloTag fusion (magenta, median = 636.6 photons) or mEos3.2 fusion (black, median = 266.8 photons) under identical imaging conditions. (**i**) Histogram of normalized occurrence *vs*. calculated localization precision when performing PALM of TOMM20 using the **6**–HaloTag fusion (magenta, median = 13.5 nm) or mEos3.2 fusion (black, median = 20.2 nm) under identical imaging conditions.

FIGURE 2

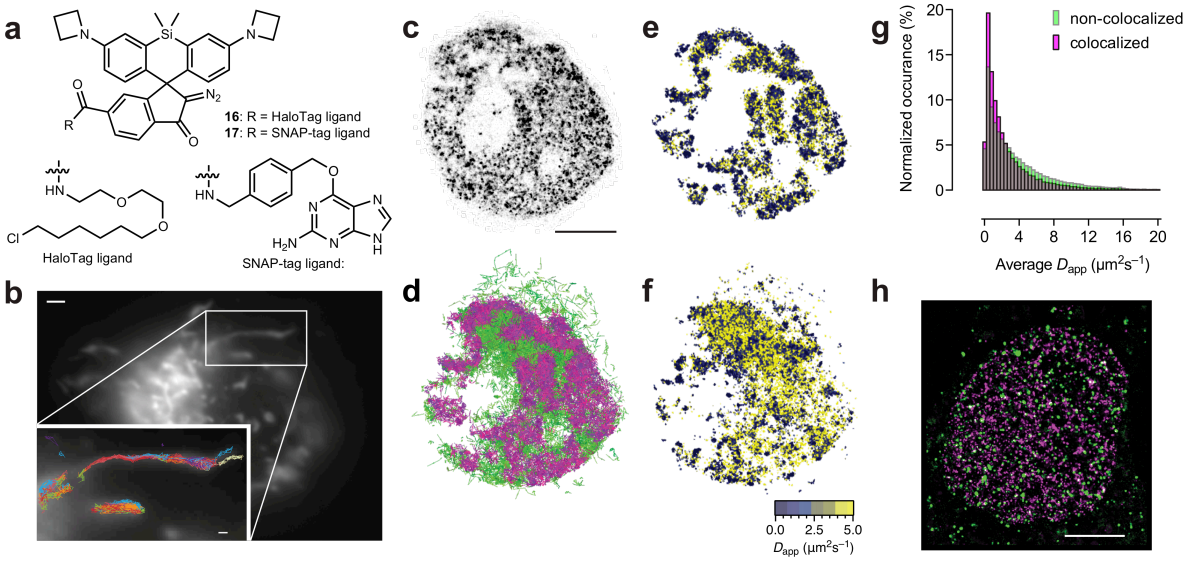

Figure 2. Multicolor imaging using photoactivatable Janelia Fluor 646 (PA-JF$_{646}$). (**a**) Structures of PA-JF$_{646}$-HaloTag ligand (**16**) and PA-JF$_{646}$-SNAP-tag ligand (**17**). (**b**) Image of U2OS cell expressing TOMM20–HaloTag and labeled with 10 nM JF$_{549}$-HaloTag ligand **8** and 10 nM PA-JF$_{646}$-HaloTag ligand **16**. The spatial distribution of the wide-field fluorescence microscopy image from JF$_{549}$-HaloTag ligand **8** resembles typical mitochondrial distribution in a cell (scale bar: 5 μm). The tracks (n=154) of single TOMM20 fusions labeled with PA-JF$_{646}$ are plotted on the averaged wide-field TOMM20-JF$_{549}$ signal (inset; scale bar: 1 μm). The majority of single molecule trajectories (>95%) colocalize with the JF$_{549}$-HaloTag signal, indicating specific labeling of PA-JF$_{646}$. (**c**–**g**) Simultaneous two-color sptPALM experiment in a live ES cell expressing histone H2B–SNAP-tag labeled with **17** and Sox2–HaloTag labeled with PA-JF$_{549}$-HaloTag ligand (**6**). (**c**) PALM image of histone H2B–SNAP-tag labeled with **17**; scale bar: 5 μm. (**d**) Single-particle trajectories of Sox2–HaloTag that are colocalized with histone H2B–SNAP-tag (6272 trajectories, magenta) or non-colocalized with histone H2B–SNAP-tag (7081 trajectories, green). (**e**) Apparent diffusion coefficient map of colocalized fraction of Sox2. (**f**) Apparent diffusion coefficient map of non-colocalized fraction of Sox2. (**g**) Histogram of normalized occurrence vs. apparent diffusion coefficient calculated for each step in the colocalized and non-colocalized Sox2 trajectories. (**h**) Overlay of the PALM image of Htt84Q–mEos3.2 clusters with the PALM image of histone H2B–HaloTag labeled with **16**. The PALM images were simultaneously recorded and are each composed of 10,000 consecutive frames. The 128,740 detected mEos3.2 molecules (green) and the 739,964 PA-JF$_{646}$ molecules (magenta) are displayed according to their localization full-width at half-maximum. The median number of detected photons per mEos3.2 molecule per frame was 115.6, and the median number of detected photons per PA-JF$_{646}$ molecule per frame was 757.6. The median calculated localization error for mEos3.2 was 34.5 nm, and for PA-JF$_{646}$ was 21.3 nm. Scale-bar: 5 μm.

SUPPLEMENTARY FIGURE 1

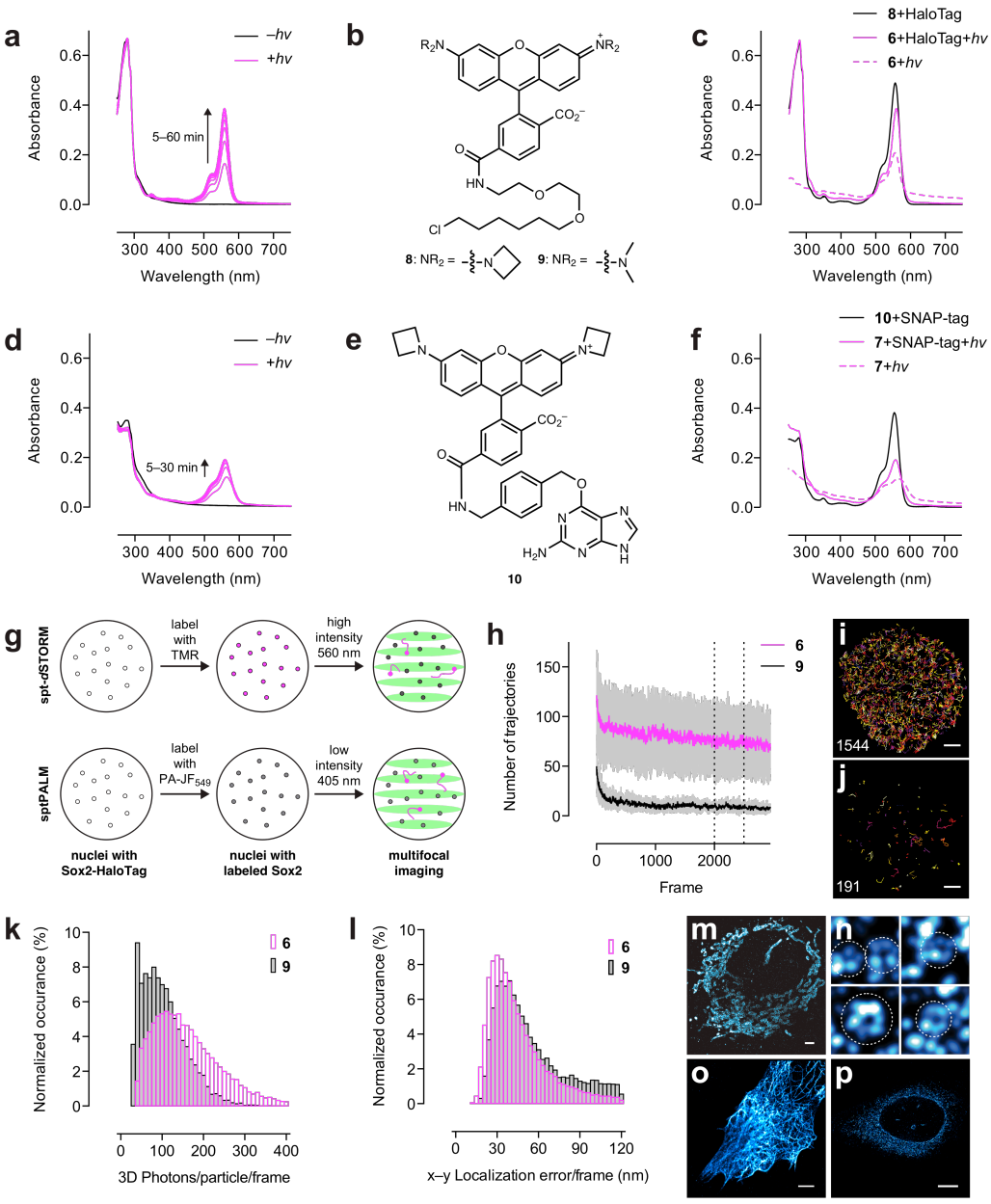

Supplementary Figure 1. Performance of PA-JF$_{549}$. (**a**) Absorbance spectrum of PA-JF$_{549}$-HaloTag ligand (**6**) bound to HaloTag protein before (–*hv*, black line) and after photoactivation (365 nm; +*hv*, magenta lines). (**b**) Structure of JF$_{549}$-HaloTag ligand (**8**) and TMR-HaloTag ligand (**9**). (**c**) Comparison of the absolute absorbance spectrum of **8** (5 μM) incubated with HaloTag protein (black) with the absorbance spectrum of **6** (5 μM) incubated with (magenta) or without (dashed magenta) HaloTag protein and then exhaustively photoconverted with 365 nm light. (**d**) Absorbance spectrum of PA-JF$_{549}$-SNAP-tag ligand (**7**) bound to HaloTag protein before (–*hv*, black line) and after photoactivation (365 nm; +*hv*, magenta lines). (**e**) Structure of JF$_{549}$-SNAP-tag ligand (**10**). (**f**) Comparison of the absolute absorbance spectrum of **10** (5 μM) incubated with SNAP-tag protein with the absorbance spectrum of **7** (5 μM) incubated with (magenta) or without (dashed magenta) SNAP-tag protein and then exhaustively

photoconverted with 365 nm light. (**g**) Cartoon showing experimental workflow of spt-*d*STORM experiment (top) and sptPALM experiment (bottom). ES cells expressing HaloTag–Sox2 were labeled to saturation with PA-JF_{549} ligand **6** or TMR-HaloTag ligand **8** and imaged on a multifocus microscope, which allows simultaneous imaging of 9 focal planes across an axial depth of ~4 μm. (**h**) Plot of the number of single molecule trajectories measured per frame in ES cell expressing HaloTag–Sox2 labeled with PA-JF_{549} ligand **6** (sptPALM mode, magenta) or the commercial TMR-HaloTag ligand (**9**; spt-*d*STORM mode, black); n = 5 cells for each ligand; s.d. shown in gray. (**i–j**) Image of cumulative single-particle tracks imaged for frames 2000-2500 (between dashed lines in **h**; only trajectories observed in >5 successive frames shown); lower left: number of trajectories measured; lower right: scale bars: 2 μm. (**i**) Cell labeled with PA-JF_{549} ligand **6** (1544 trajectories)**.** Cell labeled with standard TMR ligand **9** (191 trajectories). (**k–l**) Statistics from 3D tracking experiments (shown in **g–j**) in ES cells expressing HaloTag–Sox2 and labeled with **6** or **9**. (**k**) Histogram of normalized occurrence *vs*. photons/particle/frame using labels **6** (magenta) or **9** (black). (**l**) Histogram of normalized occurrence *vs*. particle localization/frame using labels **6** (magenta) or **9** (black). (**m**) PALM image of U2OS cells expressing TOMM20–mEos3.2 fusions. Scale-bar: 2 μm. The 195,422 detected molecules are displayed according to their localization full-width at half-maximum. The median calculated localization error was 20.2 nm. (**n**) Zoom-in of PALM image of U2OS cell expressing clathrin–HaloTag fusions and labeled with ligand **6**.The full-chip image is composed of 1,048,575 drift-corrected localizations with a median localization error of 10.8 nm. The data shows the expected ring structure of clathrin; each subpanel is 1 μm^2. (**o**) PALM image of U2OS cell expressing ensconsin–HaloTag fusions and labeled with ligand **6**. The image is composed of 445,242 localizations with a median calculated localization error of 28.7 nm. Scale-bar: 5 μm. (**p**) PALM image of U2OS cell expressing Sec61β–HaloTag fusions and labeled with ligand **6**. The image is composed of 29,356 localizations with a median calculated localization error of 20.9 nm. Scale bar: 5 μm.

SUPPLEMENTARY FIGURE 2

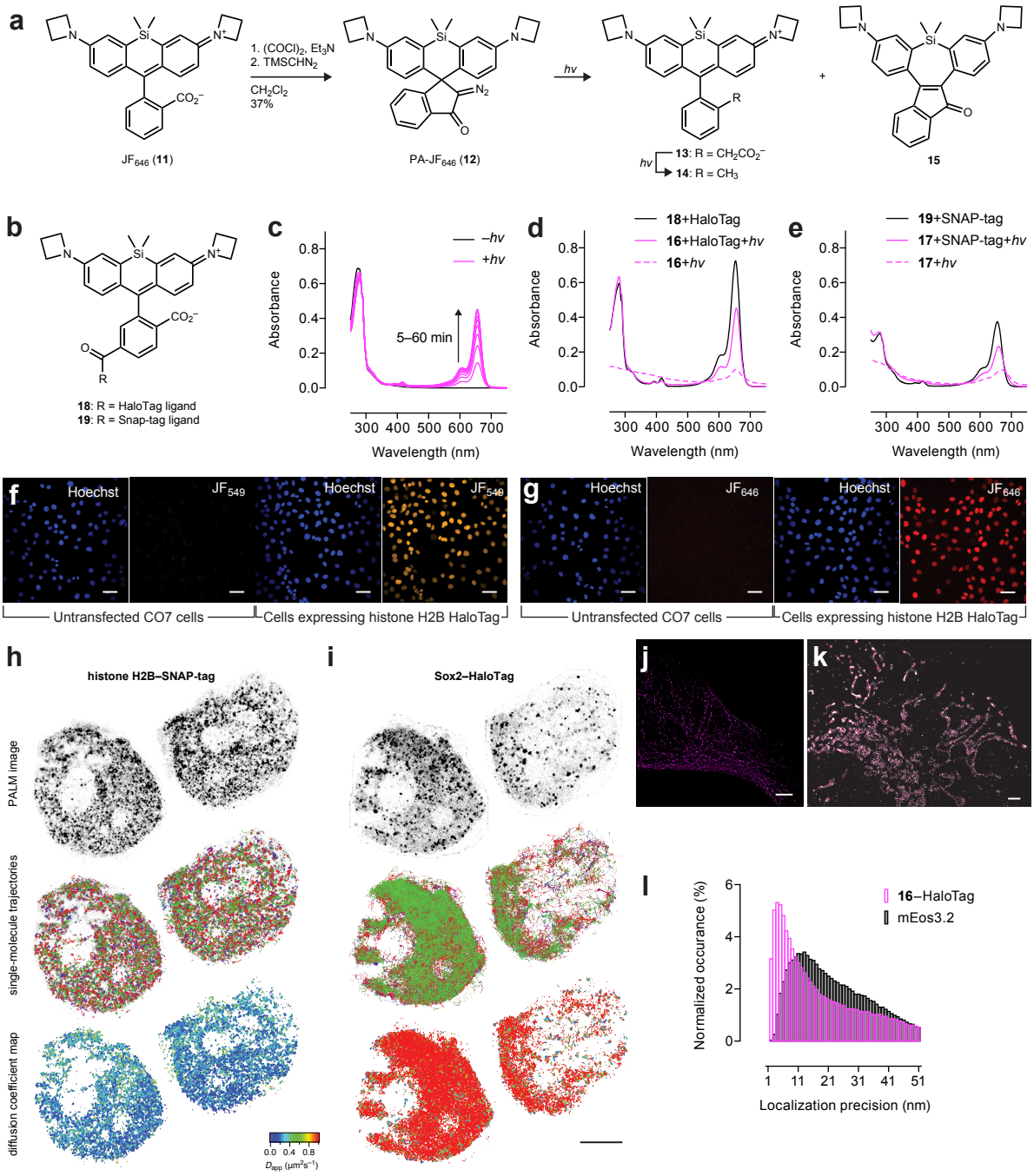

Supplementary Figure 2. Utility of PA-JF$_{646}$ (**a**) Synthesis and photochemistry of PA-JF$_{646}$. Treatment of JF$_{549}$ (**11**) with oxalyl chloride and TMS diazomethane yields PA-JF$_{646}$ (**12**). Photoconversion (365 nm) yields only a trace amount of both the phenylacetic derivative (**13**; <1%) and methyl-substituted JF$_{549}$ (**14**; 4%); the major product is the indanone **15** (24%). (**b**) Structure of JF$_{646}$-HaloTag ligand **18** and JF$_{646}$-SNAP-tag ligand **19**. (**c**) Absolute absorbance spectrum of PA-JF$_{646}$-HaloTag ligand (**16**) bound to HaloTag protein before (*–hv*, black line) and after photoactivation (365 nm; *+hv*, magenta lines). (**d**)

Comparison of the absolute absorbance spectrum of **18** (5 μM) incubated with HaloTag protein (black) with the absorbance spectrum of **16** (5 μM) incubated with (magenta) or without (dashed magenta) HaloTag protein and then exhaustively photoconverted with 365 nm light. (**e**) Comparison of the absolute absorbance spectrum of **19** (5 μM) incubated with SNAP-tag protein (black) with the absorbance spectrum of **17** (5 μM) incubated with (magenta) or without (dashed magenta) SNAP-tag protein and then exhaustively photoconverted with 365 nm light. (**f**–**g**) Evaluation of background staining of HaloTag ligands **6** and **16**. COS7 cells expressing no fusion protein (left panels) or a histone-H2B–HaloTag fusion (right panels) were fixed, stained with HaloTag ligand (100 nM; 30 min) and Hoechst 33342 (5 μg/mL), photoactivated (405 nm), and then imaged using the same settings. Scale bars: 50 μm. (**f**) JF_{549}-HaloTag ligand **6**. (**g**) JF_{646}-HaloTag ligand **16**. (**h**–**i**) Two live ES cells expressing histone H2B–SNAP-tag labeled with PA-JF_{646}-SNAP-tag ligand (**17**) and Sox2–HaloTag labeled with PA-JF_{549}-HaloTag ligand (**6**). Upper images show localization microscopy image (PALM), center images show cumulative single-particle trajectories, and lower images show apparent diffusion coefficient map. Scale bar: 5 μm. (**h**) Images from histone H2B–SNAP-tag labeled with **17**. (**i**) Images from Sox2–HaloTag labeled with **6**. (**j**) PALM image of U2OS cell expressing vimentin–HaloTag fusions and labeled with ligand **16**. The image is composed of 151,808 localizations with a median calculated localization error of 20.4 nm. Scale-bar: 5 μm. (**k**) PALM image of U2OS cell expressing TOMM20–HaloTag fusions and labeled with ligand **16**. The PALM image is composed of 203,015 detected molecules. The median calculated localization error was 13.8 nm. Scale-bar: 2 μm. (**l**) Histogram of normalized occurrence *vs*. calculated localization precision when performing PALM of TOMM20 using the **16**–HaloTag fusion (magenta, median = 13.8 nm) or mEos3.2 fusion (black, median = 20.2 nm).

SUPPLEMENTARY VIDEO LEGENDS

Supplementary Video 1. One-photon activation (405 nm) of an ES cell expressing Sox2–HaloTag labeled with PA-JF_{549}-HaloTag ligand.

Supplementary Video 2. Two-photon activation (800 nm; spelling "HHMI") in a HeLa cell expressing histone H2B-HaloTag labeled with PA-JF_{549}-HaloTag ligand followed by full-field one-photon activation (405 nm).

Supplementary Video 3. A fixed U2OS cell expressing ensconsin–HaloTag labeled with PA-JF_{549}-HaloTag ligand and imaged in PALM mode with constant excitation light (561 nm) without activation light (405 nm, 1000 frames; "OFF") and with activation light (405 nm, 1000 frames; "ON").

Supplementary Video 4. Comparison of sptPALM in ES cells expressing Sox2–mEos3.2 or Sox2–HaloTag labeled with JF_{549} or JF_{646}.

Supplementary Video 5. Side-by-side comparison of 3D single-particle tracking (spt) experiments in an ES cell expressing Sox2–HaloTag labeled with TMR HaloTag ligand (left) in spt-*d*STORM mode or PA-JF_{549} (right) in sptPALM mode.

Supplementary Video 6. 3D PALM imaging of cell expressing Sec61β–HaloTag fusions and labeled with PA-JF_{549}-HaloTag ligand.

Supplementary Video 7. One-photon activation (405 nm) of an ES cell expressing GFP–HP1 (green) and Sox2–HaloTag labeled with PA-JF_{646}-HaloTag ligand (magenta).

REFERENCES

1 Lavis, L.D. & Raines, R.T. Bright ideas for chemical biology. *ACS Chem. Biol.* **3**, 142–155 (2008).

2 Lavis, L.D. & Raines, R.T. Bright building blocks for chemical biology. *ACS Chem. Biol.* **9**, 855–866 (2014).

3 Keppler, A. *et al.* A general method for the covalent labeling of fusion proteins with small molecules in vivo. *Nat. Biotechnol.* **21**, 86-89 (2002).

4 Xue, L., Karpenko, I.A., Hiblot, J. & Johnsson, K. Imaging and manipulating proteins in live cells through covalent labeling. *Nat. Chem. Biol.* **11**, 917-923 (2015).

5 Grimm, J.B. *et al.* A general method to improve fluorophores for live-cell and single-molecule microscopy. *Nat. Methods* **12**, 244–250 (2015).

6 Grimm, J.B. *et al.* Synthesis of a far-red photoactivatable Si-rhodamine for super resolution microscopy. *Angew. Chem. Int. Ed.* **55**, 1723–1727 (2016).

7 Grimm, J.B. *et al.* Carbofluoresceins and carborhodamines as scaffolds for high-contrast fluorogenic probes. *ACS Chem. Biol.* **8**, 1303-1310 (2013).

8 Belov, V.N., Wurm, C.A., Boyarskiy, V.P., Jakobs, S. & Hell, S.W. Rhodamines NN: A novel class of caged fluorescent dyes. *Angew. Chem. Int. Ed.* **49**, 3520-3523 (2010).

9 Belov, V.N. *et al.* Masked rhodamine dyes of five principal colors revealed by photolysis of a 2-diazo-1-indanone caging group: Synthesis, photophysics, and light microscopy applications. *Chem. Eur. J.* **20**, 13162-13173 (2014).

10 Habuchi, S., Tsutsui, H., Kochaniak, A.B., Miyawaki, A. & Van Oijen, A.M. mKikGR, a monomeric photoswitchable fluorescent protein. *PloS one* **3**, e3944 (2008).

11 Epling, G.A. & Lopes, A. Fragmentation pathways in the photolysis of phenylacetic acid. *J. Am. Chem. Soc.* **99**, 2700-2704 (1977).

12 Los, G.V. *et al.* HaloTag: A novel protein labeling technology for cell imaging and protein analysis. *ACS Chem. Biol.* **3**, 373-382 (2008).

13 Betzig, E. *et al.* Imaging intracellular fluorescent proteins at nanometer resolution. *Science* **313**, 1642-1645 (2006).

14 Zhang, M. *et al.* Rational design of true monomeric and bright photoactivatable fluorescent proteins. *Nat. Methods* **9**, 727-729 (2012).

15 Abrahamsson, S. *et al.* Fast multicolor 3D imaging using aberration-corrected multifocus microscopy. *Nat. Methods* **10**, 60-63 (2013).

16 Lee, H.D. *et al.* Superresolution imaging of targeted proteins in fixed and living cells using photoactivatable organic fluorophores. *J. Am. Chem. Soc.* **132**, 1642-1645 (2010).

17 Johnsson, K., Maurel, D., Banala, S. & Manley, S. A caged, localizable rhodamine for superresolution microscopy. *ACS Chem. Biol.* **7**, 289-293 (2011).

18 English, B.P. & Singer, R.H. A three-camera imaging microscope for high-speed single-molecule tracking and super-resolution imaging in living cells. *Proc. SPIE 9550* **Biosensing and Nanomedicine VIII**, 955008 (2015).

19 Halstead, J.M. *et al.* An RNA biosensor for imaging the first round of translation from single cells to living animals. *Science* **347**, 1367-1671 (2015).

20 Wang, S., Moffitt, J.R., Dempsey, G.T., Xie, X.S. & Zhuang, X. Characterization and development of photoactivatable fluorescent proteins for single-molecule–based superresolution imaging. *Proc. Natl. Acad. Sci. U S A* **111**, 8452-8457 (2014).

21 Preibisch, S., Saalfeld, S., Schindelin, J. & Tomancak, P. Software for bead-based registration of selective plane illumination microscopy data. *Nat. Methods* **7**, 418-419 (2010).

22 Dedecker, P., Duwe, S., Neely, R.K. & Zhang, J. Localizer: Fast, accurate, open-source, and modular software package for superresolution microscopy. *J. Biomed. Opt.* **17**, 126008 (2012).

23 Katz, Z.B. *et al.* Mapping translation 'hot-spots' in live cells by tracking single molecules of mRNA and ribosomes. *eLife* **5** (2016).

24 Vallotton, P. & Olivier, S. Tri-track: Free software for large-scale particle tracking. *Microsc. Microanal.* **19**, 451-460 (2013).

25 Mortensen, K.I., Churchman, L.S., Spudich, J.A. & Flyvbjerg, H. Optimized localization analysis for single-molecule tracking and super-resolution microscopy. *Nat. Methods* **7**, 377-381 (2010).